Scientific paper

The Formation of Passive Layers on Zinc Based Platings

Ali Tuncay Ozyilmaz,[1]* Gul Ozyilmaz[1] and Ismail Hakki Karahan[2]

[1] *University of Mustafa Kemal, Faculty of Arts and Sciences, Department of Chemistry, 31000 Hatay-Turkey*

[2] *University of Mustafa Kemal, Faculty of Arts and Sciences, Department of Physics, 31000 Hatay-Turkey*

** Corresponding author: E-mail: atuncay@mku.edu.tr*
Tel.: + 90 326 245 58 45 fax: + 90 326 245 58 67

Received: 23-06-2016

Abstract

Zinc-iron (ZnFe) and zinc-iron-cobalt (ZnFeCo) platings were achieved on carbon steel applying 3 mA current values. Then, oxalate (OX) and tartrate (Tart) passive layers obtained in sodium oxalate and sodium tartrate medium were formed on carbon steel, ZnFe and ZnFeCo plated carbon steel. SEM images showed that the passive layers on CS, CS/ZnFe and CS/ZnFeCo electrodes exhibited different crystal structures. Corrosion tests revealed that the ZnFeCo particles provided a significant barrier efficiency on CS layer when compared with ZnFe alloy plating. Furthermore, OX layers on ZnFe and ZnFeCo plated carbon steel electrodes exhibited better physical barrier behavior on than those of Tart layers in longer periods

Keywords: Alloy coatings, zinc, EIS, electrodeposition, passivation, corrosion protection

1. Introduction

Zinc plating provides good protection to underlying iron based substrates. Generally metallic zinc plating provides cathodic protection as a sacrificial anode on the base metal.[1,2] Recently, there has been increasing interest in the use of electrodeposited zinc alloys against corrosion. They have been considered as alternative material instead of zinc coating on iron and steel substrates. These alloy platings are usually a combination of zinc and an 'iron group' metal. ZnFe and ZnFeCo coatings have attracted considerable attention in the automotive industry, because they combine high corrosion resistance with excellent mechanical performance. In particular, because electrodeposited ZnFe alloy coatings possess several superior properties such as excellent paintability, good welding properties and good corrosion resistance.[3–10] At the same time, zinc based coating surfaces are still coated with thin chromate or phosphate layers. There have been several studies on the application of chromatings and phosphate coatings to improve the corrosion resistance of certain coatings used in automotive industry, industrial pipes and household items. These coatings have wide range of applications due to their significant physical properties.[11–13] However, they do not last for longer period of time and can be source of lead pollution. Consequently, the corrosion performances of ZnFe and ZnFeCo coatings have been improved by insoluble layers and subsequent organic coatings. [14–15]

On the other hand, conductive polymers have been an interesting subject of research. They are of primary importance in a wide variety of scientific and industrial sectors. Some of their important properties are electrical conductivity, electroactivity, electrochromism, environmental stability, chemical stability and corrosion inhibitive property.[16–24] Yet, there is an oxidation phase of the substrate electrode prior to the electropolymerization process. This phase leads to the formation of a passive layer on the electrode surface. The dissolution of the substrates occurs in proper electrolyte medium, which is required to generate a suitable surface for the deposition of the conducting polymers. Camalet et al.[25] obtained good results in corrosion protection of mild steel with polyaniline coating synthesized in oxalic acid, which leads to the formation of a passive layer on the carbon steel substrate. In our earlier work,[26] it was found that the passivation of the ZnCo alloy surface was necessary for the homogenous polymer film synthesis prior to monomer oxidation and film growth.

In this study, passive layers were achieved electrochemically on carbon steel (CS), zinc-iron alloy plated car-

bon steel (CS/ZnFe) and zinc-iron-cobalt alloy plated carbon steel (CS/ZnFeCo) in sodium oxalate (NaOX) and sodium tartrate (NaTart) medium, in order to compare the properties of passive layers obtained in different electrolyte solutions. The synthesis of oxalate (OX) and tartrate (Tart) layers was obtained on CS, CS/ZnFe and CS/ZnFeCo electrodes including an amount of them, which enhances the passivation process. The corrosion performance of CS, CS/ZnFe and CS/ZnFeCo electrodes with and without OX or Tart layer was investigated in 3.5% NaCl and compared with the AC impedance diagrams and anodic polarization curves.

2. Materials and Methods

Sodium oxalate and sodium tartrate solutions were prepared using distilled water and all experiments were carried out at room temperature open to the atmosphere. In this study, all electrochemical experiments were performed in a single compartment cell with three electrode configurations. The reference electrode was an Ag(s)/AgCl(s)/Cl^{-1} (3 mol L^{-1}, KCl) electrode and the counter electrode was a platinum sheet with a surface area of 0.36 cm^2. A CHI 660B model digitally controlled electrochemical analyzer (serial number: A1420) was used in electrochemical experiments. All of the potential values were referred to the Ag(s)/AgCl(s)/Cl^{-1} (3 mol L^{-1}, KCl) electrode. The working electrode was a carbon steel surface (MS) measuring 0.350 cm in diameter and with the following composition (wt%): C (0.0561), Mn (0.4498), Si (0.1408), S (0.0036), P (0.0036) and Fe (balance). Carbon steel electrodes were embedded in a thick polyester block. In order to remove any existing passive film, the surface of working electrodes was polished with the help of grade emery paper up to 1200 prior to each experiment and before electrodeposition, rinsed in 1:1 ethanol acetone mixture, washed with bi-distilled water and subsequently dried.

Among the five different current values (1.0; 2.0; 3.0; 4.0 and 5.0 mA) applied for electroplating, applying 3 mA current value which had highest corrosion performance, zinc-iron (ZnFe) and zinc-iron-cobalt (ZnFeCo) platings were successfully deposited on carbon steel (CS) with chronopotentiometry technique. ZnFe plating was carried out using a bath based on 23.14 zinc sulfate ($ZnSO_4$), 10.93 iron (II) sulfate ($FeSO_4$), 24.97 sodium citrate ($Na_3C_6H_5O$), 15.98 boric acid (H_3BO_3), 24.97 glycine by weight% at pH 4.0. In case of and ZnFeCo plating, the composition of the bath was 40.90 zinc sulfate ($ZnSO_4$), 7.87 cobalt sulfate ($CoSO_4$), 2.78 iron (II) sulfate ($FeSO_4$), 12.68 sodium citrate ($Na_3C_6H_5O$), 12.68 boric acid (H_3BO_3), 22.84 ammonium chloride (NH_4Cl) and 0.25 sodium sulfate (Na_2SO_4) by weight% at pH 5.0. The thickness of alloy platings was determined by estimation of the passing charge amount applying 3 mA constant current, while the thicknesses of CS/ZnFe and CS/ZnFeCo alloy platings were estimated to be between 3.45–4.45 μm and 3.43–4.45 μm, respectively. The counter electrode was a Pt sheet with 0.36 cm^2 surface area and all alloy platings were obtained by unstirring the solution under atmospheric condition.

Oxalate and tartrate layers were synthesized by means of cyclic voltammetry technique. These layers obtained in the 0.20 M sodium oxalate (NaOX) or 0.20 M sodium tartrate (NaTart) solutions were coated on ZnFe or ZnFeCo alloy deposited carbon steel electrode by applying a scan rate of 50 mV s^{-1}. At 21 °C, the pHs of NaOX and NaTart solutions were 7.60 and 7.43, respectively. Electrochemical impedance spectroscopy, anodic polarization curves, linear sweep voltammograms and open circuit potential- time curves were used to investigate the corrosion performance of the coatings. Using amplitude of 7 mV, Nyquist plots were recorded at instantaneous open circuit potentials for various exposure times and in the frequency range from 10^5 to 10^{-3} Hz. Scanning electron microscopy (SEM) was employed to characterize the surface morphology with JEOL JSM-5500LV Scanning electron microscope. The preferable orientations of the ZnFe and ZnFeCo deposits were determined by X-ray diffraction (XRD) analysis, with a Philips PANalytical X'Pert Pro X-ray diffractometer with CuK-α radiation (lamda = 1.5418 Å). The 2 range of 20–60° was recorded at the rate of 0.02° 2θ/0.5 s. The crystal phases were identified comparing the 2 values and intensities.

3. Results and Discussion

3. 1. The Synthesis of Zinc-Iron (ZnFe) and Zinc-Iron-Cobalt (ZnFeCo) Platings

Chronopotentiometry curves recorded for ZnFe and ZnFeCo platings obtained on carbon steel (CS) applying current of 3 mA in proper bath solution are given in Fig. 1a. Both platings were achieved in 300 seconds. The potential values obtained for ZnFe and ZnFeCo platings shifted to cathodic direction at 9.0 and 29.0 seconds. Then, the behavior of each plating baths exhibited almost constant potential value after shifting to anodic potential values in time. The cobalt presence of CS/ZnFeCo electrode was proved by a significant potential shift towards nobler values, while there was a great difference between the plating potential values of CS/ZnFe and CS/ZnFeCo electrodes.

Linear sweep voltammograms recorded for CS, CS/ZnFe and CS/ZnFeCo electrodes in 0.05 M EDTA containing 0.50 M sodium sulfate solution are given in Fig. 1b. All measurements were taken at a scan rate of 5 mV s^{-1}. There was only single anodic dissolution peak for bare CS electrode and three anodic dissolution peaks for CS/ZnFe and four anodic dissolution peaks for CS/ZnFe-

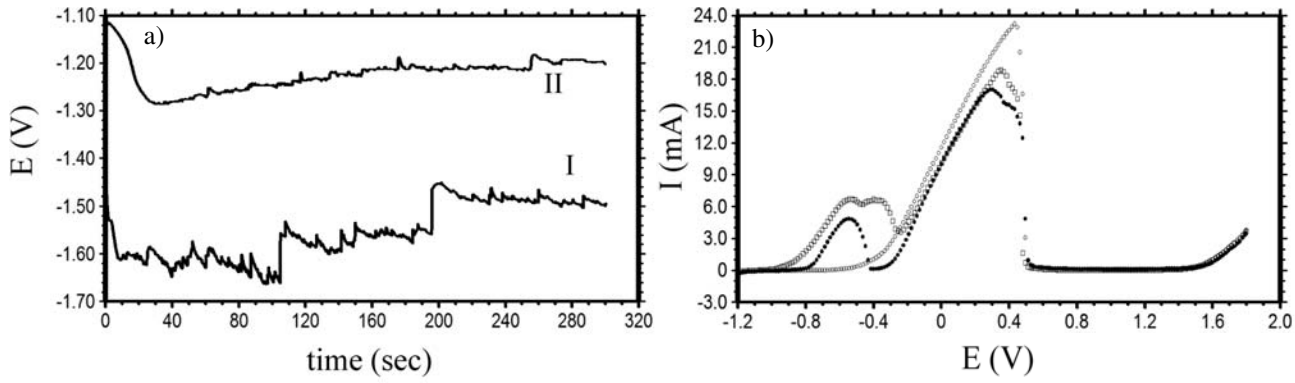

Fig. 1 . The chronopotentiometric curves of ZnFe (I) and ZnFeCo (II) alloy plated electrodes in 3.5 % NaCl solution (a) and the anodic linear sweep voltammograms (ALSVs) of CS (○), ZnFe (●) and ZnFeCo (□) electrodes in 0.50 M Na_2SO_4 + 0.05 M EDTA solution at scan rate 5 mV s^{-1} at 23.0 °C, (b), immediately after of exposure time.

Co electrodes. The peaks observed at approx. –0.54 V and 0.40 V for CS/ZnFe electrode were due to dissolution of zinc and iron by formation of zinc and iron complex with EDTA, while the same peaks for CS electrode did not appear in this potential. On the other hand, different anodic dissolution peaks at approx. –0.38 V for CS/ZnFeCo electrode were attributed to the shift to negative potential values due to the regular structure of little iron plating in crystal structure. The single peak corresponding to the anodic dissolution of iron substrate was observed at approx. +0.44 V.[27] On the other hand, there was an important difference between the heights of ZnFe and ZnFeCo alloy dissolution peaks and bare CS metallic dissolution, which could be related to the presence of alloy platings on the CS electrode. Dissolution peaks of ZnFe and ZnFeCo electrodes had low current intensities, corresponding to its significant barrier behavior against dissolution, while bare CS electrode exhibited high dissolution peak. It revealed that the ZnFe and ZnFeCo layers did not allow significant dissolution of CS electrode. Yet, the current values recorded for dissolution peaks were the lowest in presence of ZnFe plating. It was clear that, ZnFe and ZnFeCo layers provided an adequate physical protection between the base metal and corrosive environment. Consequently, zinc and cobalt oxide layers on CS/ZnFe and CS/ZnFeCo electrodes exhibited an efficient barrier property against the corrosive products.

Fig. 2Aa demonstrates a typical XRD pattern of the electrodeposited ZnFe alloy. The phases of the electrodeposited ZnFe alloy were very complicated depending on the chemical compositions.[28–29] The reflections of zinc-rich phase (JCP: 4-0831) and a æ phase were present in all investigated deposits. The electrodeposited ZnFe alloys had metastable structures and many phases coexisted over a wide range of composition. Adaniya et al. reported that the phases of electrodeposited ZnFe alloys included: η phase (100–81% Zn), δ_1/γ phase (89–70% Zn), γ phase (87–48% Zn) and α phase (62–0% Zn).[30] Only relative intensities of the two phases changed among the deposited layers with different compositions. As the Zn content in the deposits increased, the signals belonging to the η phase became more intense. Amirat et al. showed that iron incorporation leads to a dual phase alloy corresponding to a mixture of η-Zn and ζ-ZnFe phases, at 10 mA cm^{-2}. For the higher electrolytic concentration of iron in the acidic chloride electrolytic bath (Zn(II)/Fe(II) concentration rate = 1/6) the presence of ζ-phase is highlighted.[31] In presence of this study, current density and Zn(II)/Fe(II) concentration rate were attempted to be 7.8 mA cm^{-2} and 2, respectively.

Fig. 2Ab shows XRD spectra for ZnFeCo coatings on carbon steel. The Zn reflection (101) was the highest of zinc, in ZnFe and ZnFeCo coating indicating preferred orientation of this phase.[32] The pattern of the ZnFeCo coating was very different. The intensity of Zn (101) became the strongest. Winiarski[33] illustrated that the XRD results of electroplating ZnCo alloy were in agreement with the results observed in this study. In addition, this structure change in alloy plating could be explained by the different appearance in SEM images (Fig. 2Bb). The intensity of the peak corresponding Zn (101) increased progressively in ZnFeCo alloy coatings. Thus, X-ray diffraction study clearly indicates that a drastic change in the corrosion resistance of ZnFeCo coating was the consequence of change in the phase structures of the coatings. Fig. 2Ba and b shows the surface morphology of the ZnFe and ZnFeCo deposits as observed by SEM. This denoted a smooth granular deposit. As shown in Fig. 2Ba the morphology of the deposits in absence of cobalt content was small granular and more isotropic in shape. A smooth great granular uniform morphology was observed in ZnFeCo alloy deposit, which was due to the higher percentage of more noble metal in the deposit.

The synthesis of conducting polymers on oxidizable metal and their alloys have been reported in the literature recently. There is an oxidation phase of the substrate electrode prior to electropolymerization process. This phase leads to the formation of a passive layer on the electrode

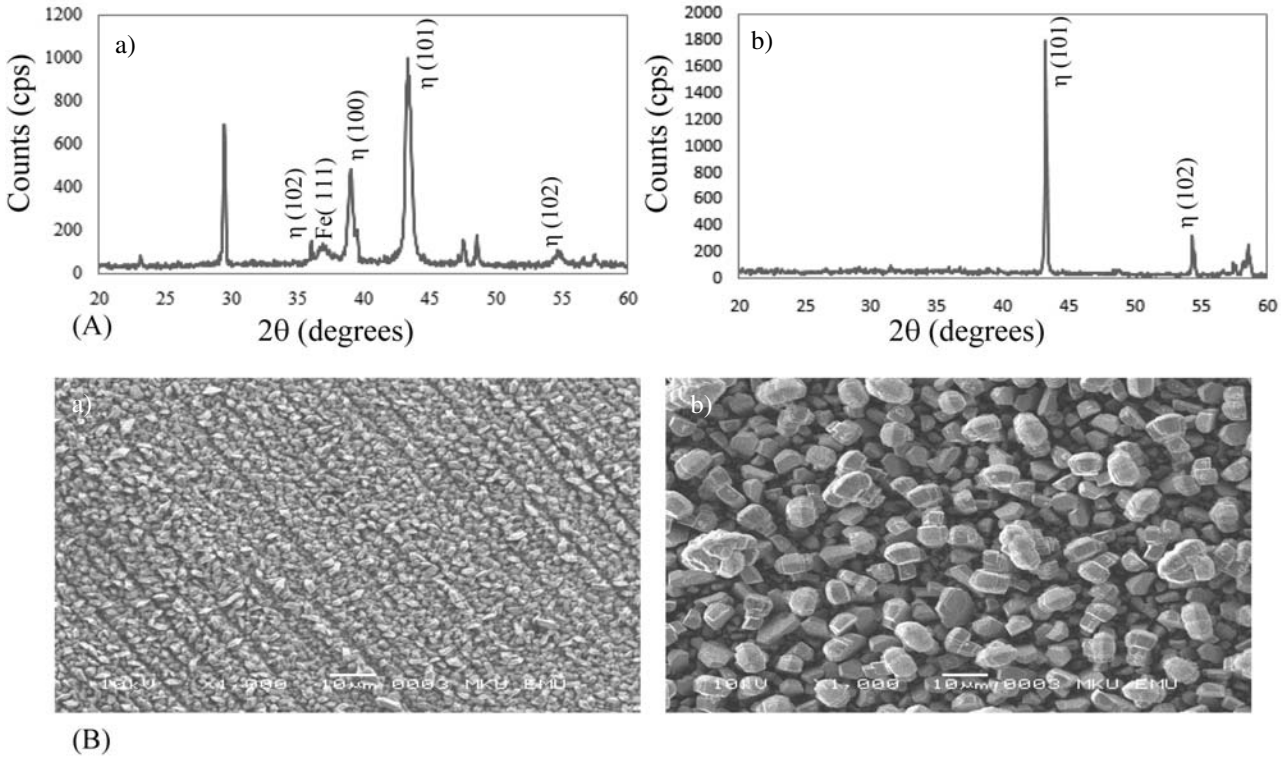

Fig. 2. X-ray diffractograms (A) and SEM images (magnification: 1000) (B) of ZnFe (a) and ZnFeCo (b) platings obtained on carbon steel applying constant current of 3 mA.

surface.[34] Passivation of especially carbon steel and iron prior to electropolymerization is very important in synthesizing homogenous and adherent polymer films. On the other hand, polymerization rate and polymer structure depend strongly on the anion type in the supporting electrolyte due to a different degree of specific adsorption of anions on mild and stainless steel. Hence, sodium oxalate and sodium tartrate aqueous solutions were used as an electrolyte to form a proper passive layer, in this study. The formulas of oxalate and tartrate anions are given below

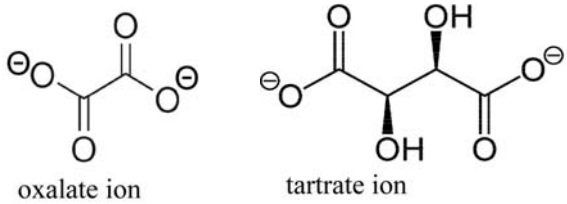

NaOX and NaTart solutions at different concentrations (0.20 M; 0.10 M; 0.05 M and 0.01 M) of were employed to obtain oxalate (OX) and tartrate (Tart) layers on CS and CS/ZnFe and CS/ZnFeCo electrodes. The OX and Tart layers formed by using an electrolyte solution at 0.20 M exhibited better barrier results against the attack of corrosion products to CS, CS/ZnFe and CS/ZnFeCo electrodes in 3.5% NaCl solution. Therefore, all results in the present study were given for 0.20 M NaOX and 0.20 M NaTart solutions.

In order to determine different processes occurring at the electrode surface, CS electrode was polarized in aqueous NaOX and NaTart solutions. Cyclic voltammograms recorded for 0.20 M NaOX and 0.20 M NaTart solutions are given in Fig. 3.

All measurements were taken at a scan rate of 50 mV s^{-1}. Twenty whole cycles were applied to obtain the oxalate and tartrate layers on CS electrode. During the first positive cycle for both NaOX and NaTart media, anodic current values remained almost constant close to zero up to 1.20 V. During the subsequent anodic potential, current values started to rise continuously due to transpassivation of CS electrode. The transpassivation potential of the CS electrode in NaTart solution shifted to negative values when compared with that of the NaOX solution. This denoted to poor interaction between carbon steel and tartrate ions due to the steric effect of hydroxide (-OH) groups in tartrate ion with respect to oxalate ions. At the reverse scan, the sharp peaks, which appeared at around –0.22 V recurred as the re-passivation peak for CS electrode. This peak was attributed to reduction from ferric compounds back to the ferrous compound on the surface.

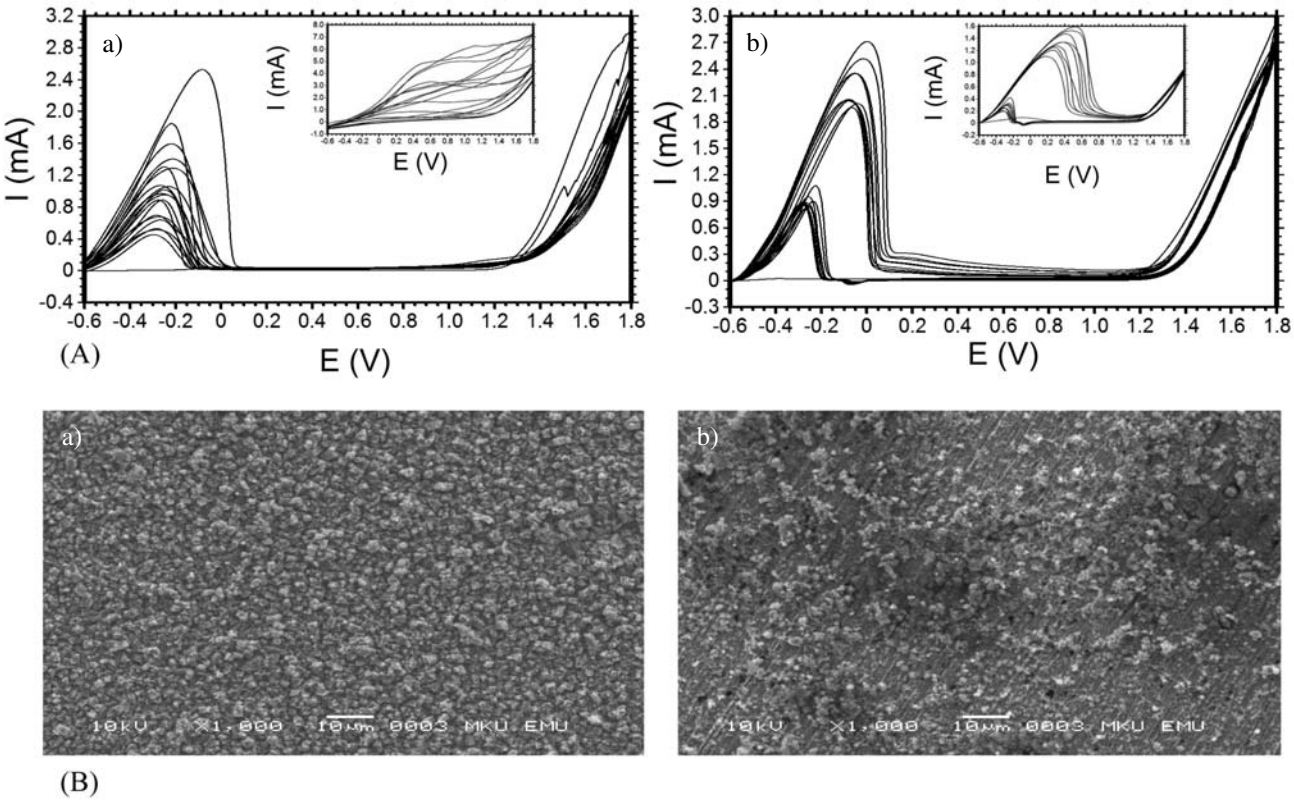

Fig. 3. Film growth curves (A) and SEM images (magnification: 1000) (B) of layers obtained on CS electrode in a) 0.20 M NaOX b) 0.20 M Na-Tart solution, scan rate: 50 mV s^{-1}.

During second and following anodic cycles, the oxidation/passivation behavior of the CS electrode was observed as well defined peak.

The passivation mechanism was based on the formation of insoluble iron (II) oxalate or iron (II) tartrate precipitations on the CS electrode. During second anodic scan, the current value of oxidation/passivation peak obtained for oxalate medium were fairly higher when compared with that of tartrate medium. This case could be explained by the inhibiting effect of huge tartrate ions. After second anodic cycle for both conditions, current values corresponding to the oxidation/passivation peak for CS electrode were found to decrease regularly with increasing scanning numbers.

In order to determine different processes occurring at the ZnFe alloy plated carbon steel (CS/ZnFe) electrode surfaces, CS/ZnFe electrode was polarized in aqueous NaOX and NaTart solutions which are referred to here as CS/ZnFeOX and CS/ZnFeTart, respectively. In order to prevent the dissolution of zinc metal, OX and Tart layers on CS/ZnFe electrode was achieved by cyclic voltammogram (CV) within potential range –0.60 to 1.80 V. CVs curves obtained in both mediums are given in Fig. 4. CVs recorded during oxalate and tartrate layer growths on CS/ZnFe electrode were significantly different from that of CS electrode. On the other hand, CVs of first scan recorded for CS/ZnFe electrode in NaOX and NaTart solutions were significantly different, while the different behavior from bare CS electrode were obtained during anodic scans with various current values. During the first positive cycle in presence of NaOX solution, active dissolution of CS/ZnFe electrode started at around –0.60 V, while the passivation of this electrode ended at around 0.51 V. Then, anodic current values remained almost constant close to zero up to 1.27 V. Anodic current values sharply started to rise due to transpassivation process and oxygen gas evolution. The first CV of CS/ZnFe in NaTart solution exhibited completely different feature from the one recorded in NaOX solution up to the commencement of transpassivation process. The passivation of CS/ZnFe electrode was observed in the narrow potential region while two oxidation/passivation peaks for CS/ZnFe electrode in NaTart solution were well defined in potential domain between –0.60 and 0.52 V. This revealed that the surface of the CS/ZnFe electrode was active in the wide potential region. The current intensity of this potential region was significantly higher when compared with that of NaOX medium. At the reverse scan, a sharp peak, which appeared at around –0.13 V was observed as the repassivation peak for CS/ZnFe electrode in NaOX solution, while this event in NaTart solution appeared as a current wave in the wide potential region.

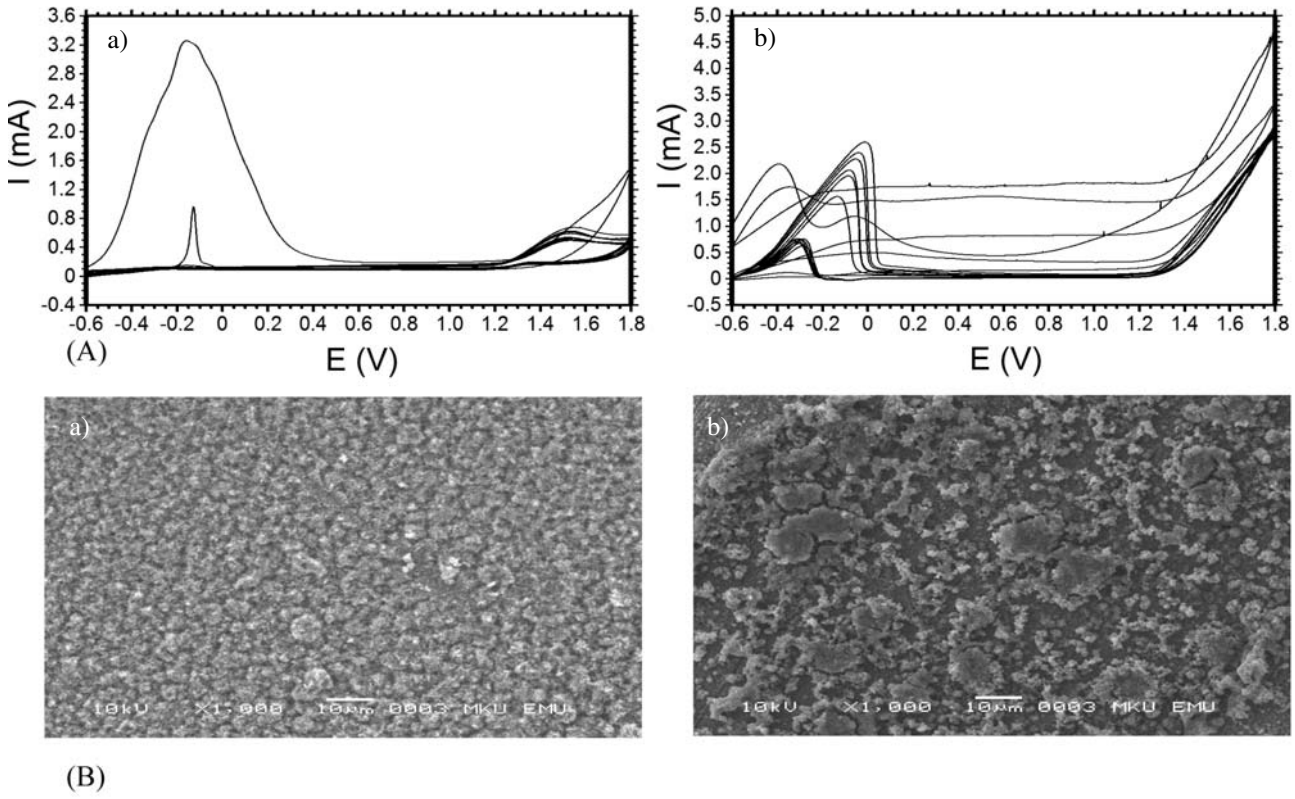

Fig. 4. Film growth curves (A) and SEM images (magnification: 1000) (B) of layers obtained on CS/ZnFe electrode in a) 0.20 M NaOX b) 0.20 M NaTart solution, scan rate: 50 mV s^{-1}.

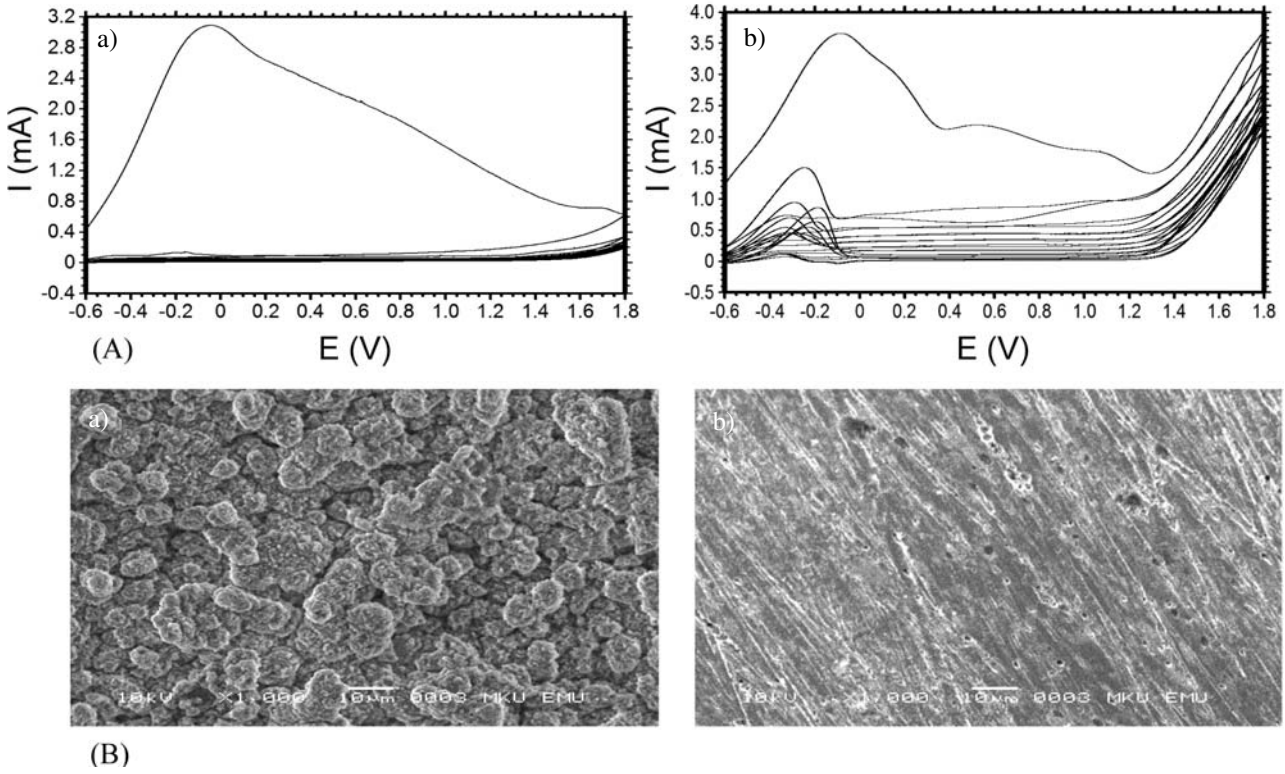

Fig. 5. Film growth curves (A) and SEM images (magnification: 1000) (B) of layers obtained on CS/ZnFeCo electrode in a) 0.20 M NaOX b) 0.20 M NaTart solution, scan rate: 50 mV s^{-1}.

This peak was attributed to reduction from ferric compounds back to the ferrous compound on the surface. However, this peak disappeared for CS/ZnFe obtained in NaOX solution due to formation of insoluble zinc oxalate and zinc oxide mono hydrate layers instead of ferric compounds on electrode surface. During second and following scans, there was not any current increase for the oxidation/passivation and repassivation process of CS/ZnFe electrode in NaOX solution, while they recurred as decreasing current values in NaTart solution.

Fig. 5 shows the cyclic voltammograms recorded for CS/ZnFeCo electrode in NaOX and NaTart electrolyte solutions. In presence of NaOX solution, high current values obtained for the formation of iron oxalate and cobalt oxalate layers made it clear that passivation of CS/ZnFeCo electrode ended during oxidation/passivation process, which could be explained by low current values which were observed during second and following scans. However, this passivation phenomenon could not be seen on the same CS/ZnFeCo electrode in NaTart solution. So, the intensities of both oxidation/passivation peaks at anodic scan and the repassivation peaks at cathodic scan were found to decrease steadily with increasing scanning numbers. After the second anodic scan, passive region was observed in the wide potential range before transpassivation process.

3. 3. Corrosion Performances of Uncoated and Coated Electrodes

The anticorrosive properties of all electrodes were evaluated in the 3.5% NaCl solution with anodic polarization curves, the open circuit potential (E_{ocp})-time curves and electrochemical impedance spectroscopy (EIS).

The Nyquist diagrams of CS, CS/ZnFe and CS/ZnFeCo electrodes recorded for 48 and 168 h of exposure times are given in Fig. 6.

Nyquist plots recorded for CS and CS/ZnFeCo electrodes consisted of only one depressed semicircle, while two different constant phase elements were observed at region ranging from high frequency to low frequency for CS/ZnFe electrode. The appearance of different constant phase elements indicated prominent differences between capacitive behavior of passive layers and the corrosion reaction on the CS/ZnFe surface. Consequently, this suggested that two different constant phase elements were observed for metal/electrolyte and plating/electrolyte interfaces. After 48 h of immersion time, the corrosion rate (I_{corr}) of alloy platings was higher than bare carbon steel due to active zinc content (Table 1).

In Nyquist curves of all electrodes, the appearance of only one capacitive semicircle could be related to the insignificant phenomena revealing a change to activate carbon steel at the metal/solution interface, after 168 h of exposure time. This indicated smaller differences between capacitive behavior of passive layers and the corrosion reaction on the surface. Consequently, this suggested that the constant phase element might be considered as two overlapping semicircles. This behavior recorded for CS electrode was discussed in detail in our previous study.[26]

In Table 1, The R_p value decreased for CS electrode, while these values obtained for CS/ZnFe and CS/ZnFeCo electrodes increased after 168 h of exposure time. In addi-

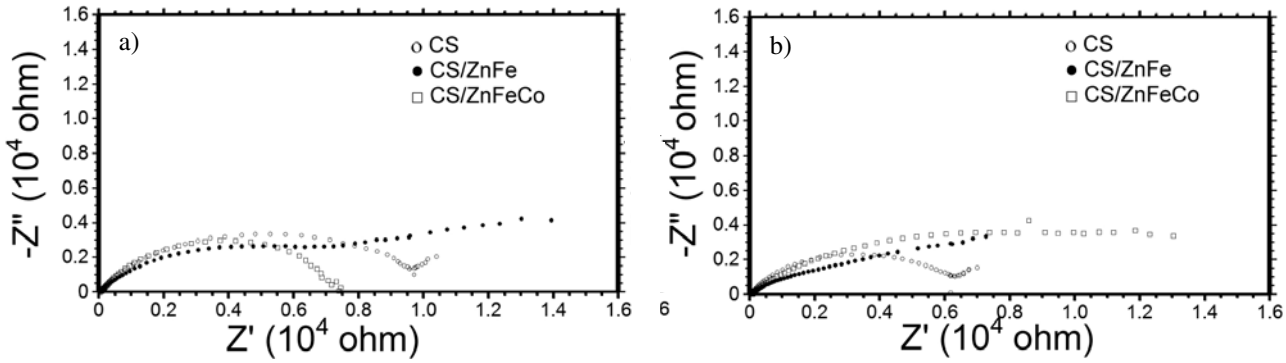

Fig. 6. The Nyquist curves of electrodes, after (a) 48 h and (b) 168 h of exposure time in 3.5% NaCl solution.

Table 1. Impedance data obtained by simulation of Fig. 6. β_a= 170 mV dec^{-1} for bare carbon steel electrode

Electrodes	t (h)	E_{ocp} (V)	R_p (Ω)	R_{ct} (Ω)	R_f (Ω)	I_{corr} (μA)	E (%)	P (%)
Uncoated CS	48	–0.669	9983	–	–	2.60	–	–
	168	–0.655	6691	–	–	3.89	–	–
CS/ZnFe	48	–0.662	8635	–	–	6.02	–	–
	168	–0.659	9368	–	–	5.55	–	67.66
CS/ZnFeCo	48	–0.768	7396	–	–	7.03	–	35.31
	168	–0.622	12966	–	–	4.01	48.40	33.00

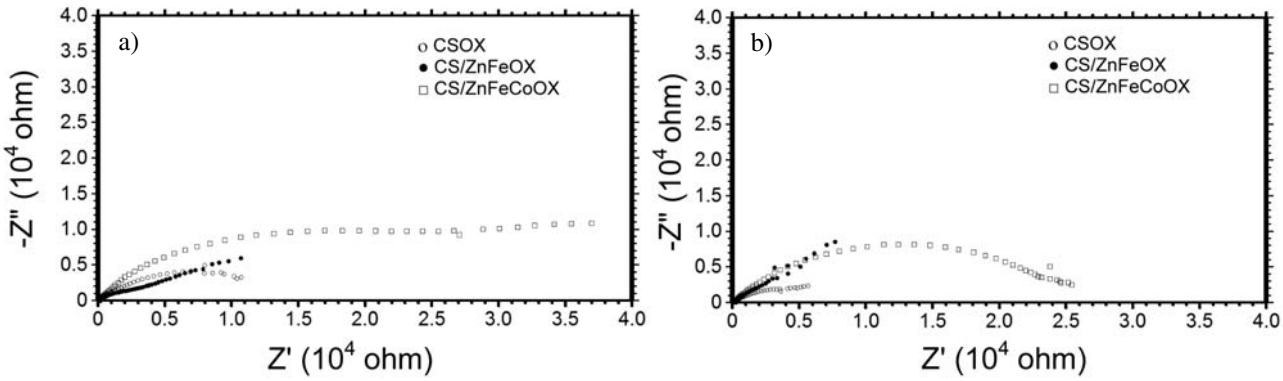

Fig. 7. The Nyquist curves of electrodes after (a) 48 h and (b) 168 h of exposure time in 3.5% NaCl solution.

tion the R_p values of CS/ZnFe and CS/ZnFeCo electrodes were significantly higher when compared with uncoated CS electrode. The increase in the R_p values recorded for CS/ZnFe and CS/ZnFeCo electrodes simply indicated that alloy coatings provided an adequate physical protection to the metal between the corrosive environment and the base metal. On the other hand, ZnFe and ZnFeCo platings on carbon steel had relatively porous film structure (Table 1) and could provide poor protection to the substrate. The total diameter of depressed semicircles obtained for each electrode was equal to R_p value. After 168 h of exposure time, the highest R_p value was obtained for the CS/ZnFeCo electrode.

The Nyquist diagrams recorded for CSOX, CS/ZnFeOX and CS/ZnFeCoOX electrodes are given in Fig. 7, for 48 and 168 h of exposure times in 3.5% NaCl solution.

In case of CSOX and CS/ZnFeOX electrodes, Nyquist plots consisted of two depressed semicircles, which could not be well resolved after 48 h of immersion time. The first region observed in the highest frequency, which was related to the resistance against corrosion, was equal to the sum total of diffusion resistance (R_d) and the charge transfer resistance (R_{ct}) within pores of alloy plating and oxalate layers for CS/ZnFeOX electrode and oxalate layer for CSOX electrode. The second semicircle for CSOX electrode was attributed to the passive layer resistance (R_{pl}) arising from iron (II) oxalate formed on the CSOX electrode, while second semicircle for CS/ZnFeOX electrode was equal to the alloy coating resistance (R_{coat}) and resistance of zinc oxalate and iron (II) oxalate layers. The total resistance values recorded for CS/ZnFeCoOX electrode consisted of one depressed semicircle ranging from high frequency to low frequency at the end of 48 h. During this time, CS/ZnFeCoOX electrode exhibited highest corrosion performance against the attack of corrosion products such as aggressive chloride ions to carbon steel electrode. After 168 h of immersion time, corrosion resistance recorded for CSOX and CS/ZnFeCoOX electrodes declined due to the fallen barrier property of oxalate layers and their permeability increased in the presence of chloride ions (Table 2).

Nyquist curve in longer periods, the exhibition of linear part, which denoted to the presence of Warburg impedance (Z_w) for CS/ZnFeOX electrode, could be attributed to the significant phenomena revealing a remarkable formation of new oxide layers on the CS/ZnFe electrode at the metal/solution interface.[35–38] This linear part recorded for CS/ZnFe electrode showed a typical charge transfer process occurring under diffusion control. So, the presence of the linear part in the lower frequency region indicated that the corrosion reaction was inhibited by mass transfer limitation. This case was related to the semi-infinite diffusion of ions at the layer/electrolyte interface.

Nyquist curves obtained for CSTart, CS/ZnFeTart and CS/ZnFeCoTart electrodes after 48 h exposure time in 3.5% NaCl solution are given in Fig. 8. There was one depressed semicircle ranging from high frequency to low frequency region for all three electrodes. After 48 h of im-

Table 2. Impedance data obtained by simulation of Fig. 7. β_a= 170 mV dec^{-1} for bare carbon steel electrode

Electrodes	t (h)	E_{ocp} (V)	R_p (Ω)	R_{ct} (Ω)	R_f (Ω)	I_{corr} (μA)	E (%)	P (%)
CS/OX	48	–0.653	24193	10094	14099	2.15	58.74	33.22
	168	–0.660	7603	–	–	6.84	12.00	82.24
CS/ZnFe/OX	48	–0.670	8590	1934	6656	6.05	–	90.20
	168	–0.741	337	–	–	–	–	–
CS/ZnFeCo/OX	48	–0.626	35209	–	–	1.48	78.99	3.07
	168	–0.618	26040	137	25903	2.00	50.21	47.17

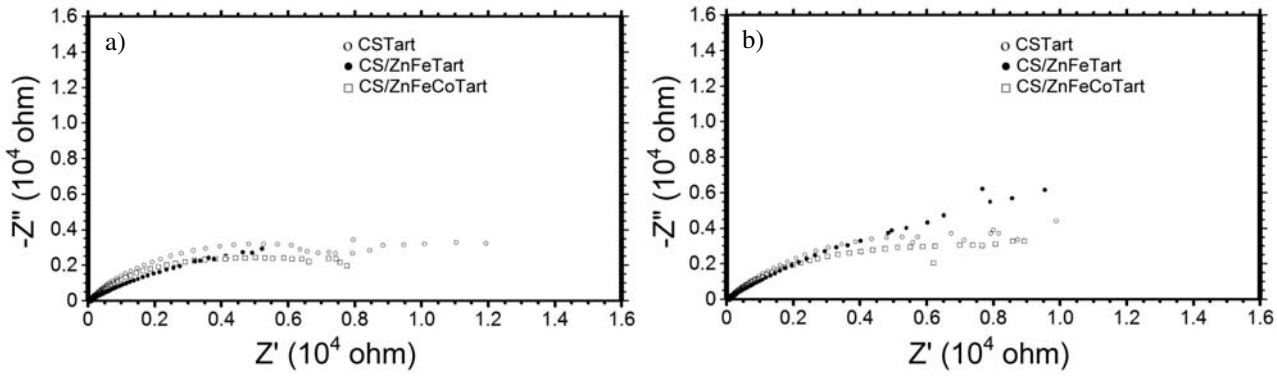

Fig. 8. The Nyquist curves of electrodes, after (a) 48 h and (b) 168 h of exposure time in 3.5% NaCl solution.

mersion time, CSTart and CS/ZnFe electrodes exhibited highest corrosion resistance against the attack of corrosion products such as aggressive chloride ions to carbon steel electrode.

The exhibition of high capacitive semicircles could be related to the significant phenomena revealing a change to passive CS and CS/ZnFe electrode at the metal/solution interface. On the other hand, in Table 3, the percent porosity value of CS/ZnFeCo electrode was lowest during this period. During 168 h of immersion time, the R_p values of all electrodes obtained in NaTart medium increased due to presence of increasing passive layers at the carbon steel surface.

The increasing values indicated that the barrier property of layers enhanced during this period and the permeability of CS and CS/ZnFe electrodes decreased in the presence of chloride ions. On the other hand, the R_p value of the CSTart electrode was significantly higher than that of CSOX electrode, while these values of CS/ZnFeTart and CS/ZnFeCoTart electrodes were significantly lower when compared with those of CS/ZnFeOX and CS/ZnFeCoOX electrodes.

Open circuit potential-time and anodic polarization curves recorded for CS, CS/ZnFe and CS/ZnFeCo electrodes in 3.5% NaCl solution are given in Fig. 9.

The open circuit potential (E_{ocp}) values of the electrodes were monitored with time (Fig. 9a). Immediately

Table 3. Impedance data obtained by simulation of Fig. 8. β_a= 170 mV dec^{-1} for bare carbon steel electrode

Electrodes	t (h)	E_{ocp} (V)	R_p (Ω)	R_{ct} (Ω)	R_f (Ω)	I_{corr} (μA)	E (%)	P (%)
CS/Tart	48	–0.678	11122	–	–	4.68	10.24	79.46
	168	–0.678	12599	–	–	4.13	46.89	38.89
CS/ZnFe/Tart	48	–0.642	11302	–	–	4.60	23.60	58.72
	168	–0.666	20032	–	–	2.60	53.23	42.53
CS/ZnFeCo/Tart	48	–0.633	8963	–	–	5.80	17.48	13.26
	168	–0.637	10743	–	–	4.84	–	98.50

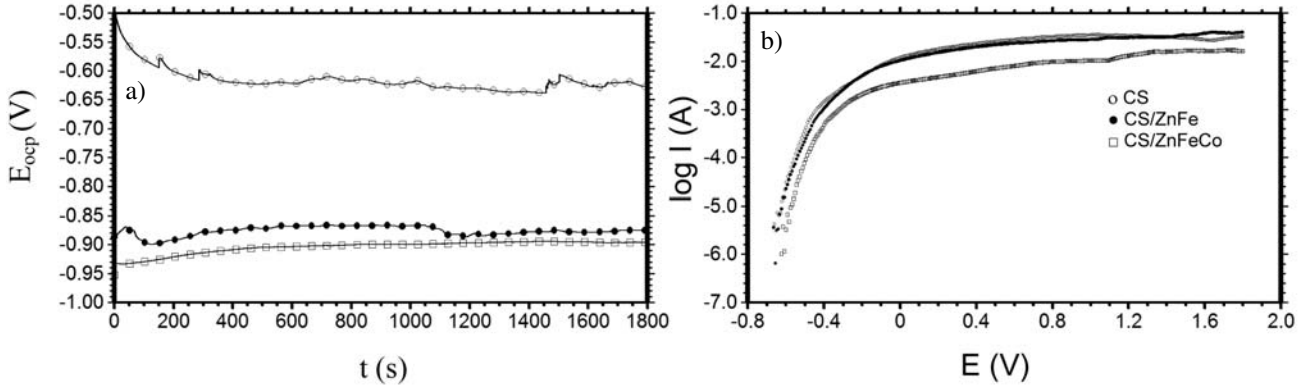

Fig. 9. The E_{ocp}-t diagrams immediately after of immersion time (a) and the anodic polarization curves after 168 h of exposure time (b) obtained for electrodes, in 3.5% NaCl solution.

after of immersion, E_{ocp} values were measured as –0.493 V, –0.887 V and –0.952 V for bare CS, CS/ZnFe and CS/ZnFeCo electrodes, respectively. E_{ocp} values of bare CS electrode shifted to negative potentials up to 1457 s of exposure time. Afterwards, E_{ocp} values remained negative in the active state, although it shifted to some anodic direction. There was not any possibility for passivation of the CS electrode surface under aggressive chloride ions condition, while its E_{ocp} value was –0.628 V, after 1800 s of immersion time. On the other hand, E_{ocp} values of CS/ZnFe and CS/ZnFeCo electrodes had more negative potential values when compared with bare CS electrode for all of immersion time. E_{ocp} values of the CS/ZnFe electrode were only slightly less positive than those of CS/ZnFeCo electrode, while their values increased in time and reached higher values. This case was attributed to remain in the passive state at sufficiently positive potentials. There was not a great difference between the E_{ocp} values of CS/ZnFe and CS/ZnFeCo electrodes, after 1800 s. Anodic polarization tests carried out on CS, CS/ZnFe and CS/ZnFeCo electrodes are shown in Fig. 9b. Although the E_{corr} value of CS/ZnFe electrode was shifted in only slightly less noble region than that of uncoated electrode, the corrosion current (I_{corr}) values were almost same with that of uncoated electrode. This observation revealed that ZnFe alloy plating provided poor corrosion protection to CS electrode. On the other hand, lowest current values recorded for CS/ZnFeCo electrode simply indicated that ZnFeCo alloy plating provided an adequate physical protection to the metal between the corrosive environment and underlying metal. In Table 1, the highest R_p value of CS/ZnFeCo electrode supported this fact, after 168 h of exposure time. In addition, the positive shift in the E_{corr} values recorded for CS/ZnFeCo electrode gave an evidence for passivation of the CS/ZnFeCo electrode surface under aggressive chloride ions condition.

In order to determine different passive layers occurring on ZnFe and ZnFeCo alloy plated carbon steel and bare carbon steel electrode surfaces were polarized in aqueous 0.20 M sodium oxalate (OX) and 0.20 M sodium tartrate (Tart) solutions.

Fig. 10 shows open circuit potential-time and anodic polarization curves recorded for CSOX, CS/ZnFeOX and CS/ZnFeCoOX electrodes in 3.5% NaCl solution. In the case of uncoated CS electrode, E_{ocp} values remained constant close to the same potential value in 1800 s. The almost constant value of this potential indicated the growth of the passive layer composed of iron oxides within the porous structure of zinc and iron oxalate layers. The ZnFeOX or ZnFeCoOX platings, which induced passivation of CS electrode was accompanied by a significant potential shift towards more noble E_{ocp} values. The active role of OX layer in corrosion protection was due to the interaction between the ZnFe or ZnFeCo plating and the oxalate resulting in initiation of CS passivation, while E_{ocp} values of the CS/ZnFeCoOX electrode were significantly nobler when compared with that of the CS/ZnFeOX electrode after 1800 s of exposure time. Anodic polarization curves obtained for CSOX, CS/ZnFeOX and CS/ZnFeCoOX electrodes after 168 h exposure time in 3.5% NaCl solution are given in Fig. 10b. In the case of CSOX sample, corrosion potential value (E_{corr}) was observed to be –0.635 V. Current values increased so rapidly that there was not any possibility for passivation of the CS electrode surface under aggressive chloride ions condition. The E_{corr} value of CS/ZnFeOX electrode (–0.606 V) shifted in the nobler region than that of CS electrode. The positive shift in the E_{corr} value for oxalate layer coated CS/ZnFeCo electrode simply indicated that oxalate layer created an important passive layer on ZnFeCo alloy plating between the corrosive environment and the base metal. This occasion supported the idea that the current values of CS/ZnFeCoOX electrode were significantly lower when compared with CSOX electrode. Yet, lowest current values in anodic polarization curves were observed for CS/ZnFeOX electrode which had strongly passive layers. These results supported the R_p values obtained in longer period that OX layers on ZnFeCo and ZnFe alloy depositions provided significantly better corrosion protection than that of OX layer on CS electrode. On the other hand, the anodic polarization curves of OX coated CS, CS/ZnFe and CS/ZnFeCo electrodes had lower current values when compared with

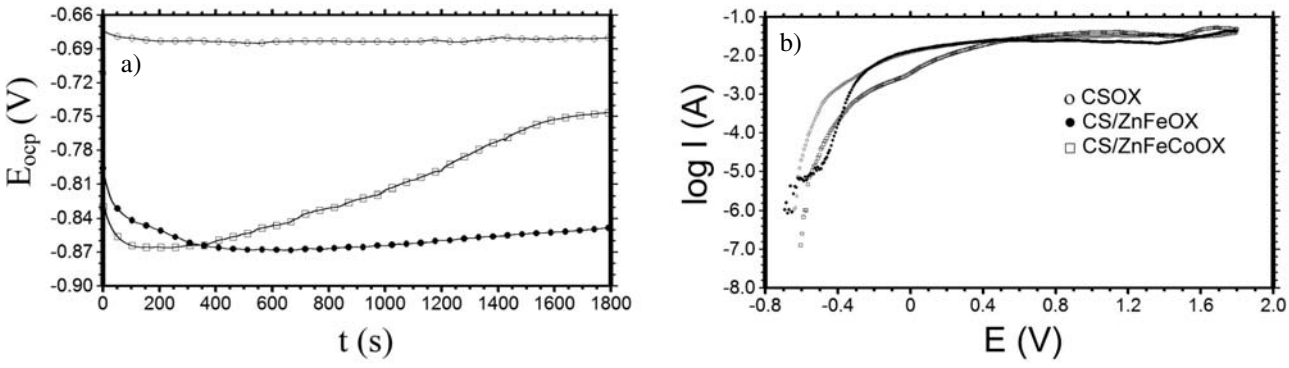

Fig. 10. The E_{ocp}-t diagrams immediately after of immersion time (a) and the anodic polarization curves after 168 h of exposure time (b) obtained for electrodes, in 3.5% NaCl solution.

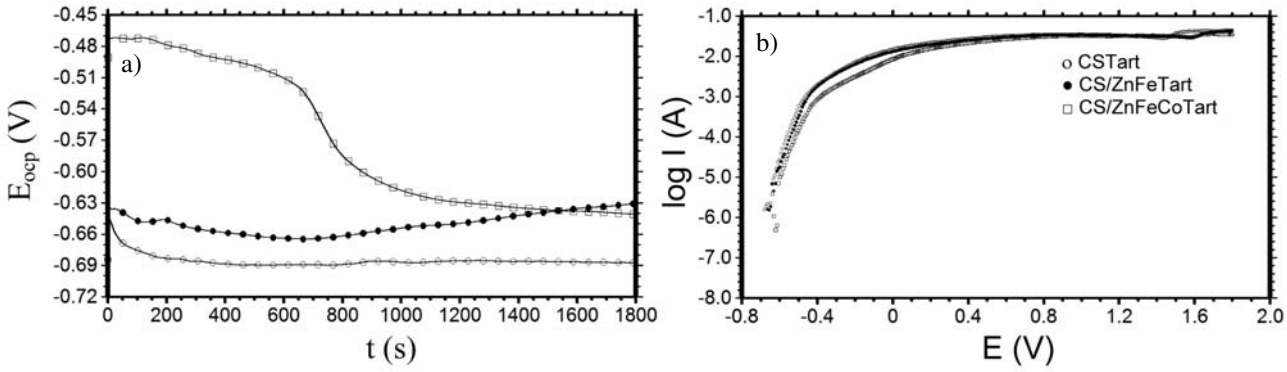

Fig. 11. The E_{ocp}-t diagrams immediately after of immersion time (a) and the anodic polarization curves after 168 h of exposure time (b) obtained for electrodes, in 3.5% NaCl solution.

those of oxalate free CS, CS/ZnFe and CS/ZnFeCo electrodes.

The open circuit potential-time and anodic polarization curves of CSTart, CS/ZnFeTart and CS/ZnFeCoTart electrodes are given in Fig. 11. It is significant that the E_{ocp} values of CS/ZnFeTart and CS/ZnFeCoTart electrodes were relatively nobler with respect to that of CSTart electrode, in 3.5% NaCl solution. Immediately after of immersion time to 3.5% NaCl solution, the surface of ZnFe and ZnFeCo plating exhibited passivation according to the formation of zinc tartrate, iron tartrate and cobalt tartrate layers. At the same time, these passive layers provided a resistance against the attack of corrosion products in time, while the E_{ocp} values of CS/ZnFeTart and CS/ZnFeCoTart electrodes were measured as –0.631 V and –0.641 V after 1800 s, respectively (Fig. 11a). In Fig. 11b, anodic polarization tests were also carried out for CSTart, CS/ZnFeTart and CS/ZnFeCoTart electrodes.

After 168 h of immersion time, E_{corr} values were –0.676 V for CSTart, –0.659 V for CS/ZnFeTart and –0.635 V for CS/ZnFeCoTart electrodes. The positive shift in the E_{corr} values for CS/ZnFeTart and CS/ZnFeCoTart electrodes indicated that ZnFeTart and ZnFeCoTart coatings provided significantly better physical protection to the CS metal between the corrosive environment and the base metal. At the same time, there were much lower current values for CS/ZnFeCoTart electrode when compared with CS/ZnFeTart electrode as well as CSTart electrode. On the other hand, CS/ZnFeOX and CS/ZnFeCoOX electrodes exhibited highest corrosion performance against the attack of corrosion products such as aggressive chloride ions to carbon steel electrode, when compared with CS/ZnFeTart and CS/ZnFeCoTart electrodes.

5. Conclusions

In this study, zinc-iron (ZnFe) and zinc-iron-cobalt (ZnFeCo) alloy platings were successfully deposited on carbon steel (CS) applying 3 mA current value. XRD and SEM results showed that ZnFe and ZnFeCo platings exhibited different crystal structures on carbon steel electrode. Then, passive layers contained oxalate and tartrate component were achieved electrochemically on carbon steel (CS), zinc-iron alloy plated carbon steel (CS/ZnFe) and zinc-iron-cobalt alloy plated carbon steel (CS/ZnFeCo) in sodium oxalate (NaOX) and sodium tartrate (NaTart) medium, respectively. The synthesis of oxalate (OX) and tartrate (Tart) layers was obtained on CS, CS/ZnFe and CS/ZnFeCo electrodes including an amount which would enable the passivation process. SEM images showed that the passive layers on CS, CS/ZnFe and CS/ZnFeCo electrodes exhibited different crystal structures. The corrosion performance of CS, CS/ZnFe and CS/ZnFeCo electrodes with and without OX or Tart layer was investigated in 3.5% NaCl and compared with the AC impedance diagrams, open circuit potential-time curves and anodic polarization curves. As a result, corrosion tests revealed that the ZnFeCo particles provided a significant barrier efficiency on CS layer when compared with ZnFe alloy plating. Furthermore, OX layers on CS, CS/ZnFe and CS/ZnFeCo electrodes exhibited better physical barrier behavior than those of Tart layers. At the same time, ZnFeOX and ZnFeCoOX coatings showed high stability and low permeability under aggressive condition and provided best anodic protection behaviour on carbon steel electrode in longer immersion periods.

6. Acknowledgements

The research project was funded by Technical Research Council of Turkey (TUBITAK), Project No: TBAG- (110T745) and The University of Mustafa Kemal in Turkey, Project No: 12220.

7. References

1. E. Kornienko, R. Ossenbrink, V. Michailov, *Corrosion Science* **2013**, *69*, 270–280.

http://dx.doi.org/10.1016/j.corsci.2012.12.013
2. K. R. Sriraman, S. Brahimi, J. A. Szpunar, J. H. Osborne, S. Yue, *Surface and Coatings Technol.* **2013**, 224, 126–137 http://dx.doi.org/10.1016/j.surfcoat.2013.03.010
3. Z. F. Lodhi , J. M. C. Mol, A. Hovestad, L. 't Hoen-Velterop, H. Terryn, J. H. W. de Wit, *Surf. Coat. Tech.*, **2009,** *203*, 1415–1422. http://dx.doi.org/10.1016/j.surfcoat.2008.11.019
4. A. Rafiee, K. Raeissi,; M. A. Golozar, *Transactions of the Institute of Metal Finishing.* **2014**, *92*, 115–120. http://dx.doi.org/10.1179/0020296713Z.000000000122
5. Mortaga M. Abou-Krisha, *Appl. Surface Sci*. **2005**, *252*, 1035–1048. http://dx.doi.org/10.1016/j.apsusc.2005.01.161
6. J. B. Bajat, S. Stanković, B. M. Jokić, S.I. Stevanović, *Surface and Coatings Technol*. **2010**, *204*, 2745–2753. http://dx.doi.org/10.1016/j.surfcoat.2010.02.032
7. J. Mahieu, K. De Wit, A. De Boeck, B. C. De Cooman, *J. Materials Eng. and Performance.* **1999**, *8(5),* 561–570. http://dx.doi.org/10.1007/s11665-999-0010-x
8. A. Bai, C. Hu, *Electrochemistry Communications*, **2003,** *5*, 78–82. http://dx.doi.org/10.1016/S1388-2481(02)00540-4
9. M. M. Abou-Krisha, F. H. Assaf, S.A. El-Naby, *J. Coatings Technol. Research.* **2009**, *6(3)*, 391–399. http://dx.doi.org/10.1007/s11998-008-9134-4
10. S. Amirat, R. Rehamnia, M. Bordes, J. Creus, *Materials and Corrosion.* **2013**, *64*, 328–334. http://dx.doi.org/10.1002/maco.201106290
11. M. R. El-Sharif, Y. J. Su, C. U. Chisholm, A. Watson, *Corros. Sci.*, **1993**, *35*, 1259–1265. http://dx.doi.org/10.1016/0010-938X(93)90346-I
12. A. A. O. Magalhães, I .C. P. Margarit, O. R. Mattos, *J Electroanal.Chem.* **2004**, *572*, 433–440.
13. M. H. Sohi, M. Jalali, *J. Mater. Process. Tech.* **2003**, *138*, 63–66. http://dx.doi.org/10.1016/S0924-0136(03)00050-5
14. C. K. Tan, D. J. Blackwood, *Corrosion Sci.* **2003,** *45*, 545–557. http://dx.doi.org/10.1016/S0010-938X(02)00144-0
15. J. I. Martins, T. C. Reis, M. Bazzaoui,E. A. Bazzaoui and L. Martins, *Corros. Sci.* **2004**, *46*, 2361–2381. http://dx.doi.org/10.1016/j.corsci.2004.02.006
16. G. M. Spinks, A. J. Dominis, G. G. Wallace, D. E. Tallman, *J. Solid State Electrochem.* **2002**, *6*, 85–100. http://dx.doi.org/10.1007/s100080100211
17. A. T. Ozyilmaz, G. Ozyilmaz, N. Çolak, *Surface and Coatings Technol.* **2006**, *201*, 2484–2490. http://dx.doi.org/10.1016/j.surfcoat.2006.04.008
18. A. Olad, H. Rasouli, *J. Appl. Polymer Sci*. **2010**, *115*, 2221–2227. http://dx.doi.org/10.1002/app.31320
19. K. R. Prasad, N. Munichandraiah, *Synthetic Metals.* **2002**, *130*, 17–26. http://dx.doi.org/10.1016/S0379-6779(02)00099-1
20. M. Kraljić, Z. Mandić, Lj. Duić, *Corrosion Sci*. **2003**, *45*, 181–198. http://dx.doi.org/10.1016/S0010-938X(02)00083-5
21. D. Sazou, C. Georgolios, *J. Electroanal. Chem*. **1997**, *429*, 81–93. http://dx.doi.org/10.1016/S0022-0728(96)05019-X
22. A. Yagan, N. O. Pekmez, A. Yýldýz, *Electrochimica Acta*, **2006**, *51*, 2949–2955. http://dx.doi.org/10.1016/j.electacta.2005.08.029
23. A. T. Ozyilmaz, M. Erbil, B. Yazýcý, *Current Applied Physics.* **2006**, *6*, 1–9. http://dx.doi.org/10.1016/j.cap.2004.06.027
24. J. L. Camalet, J. C Lacroix, S. Aeiyach, K. Chane-Ching, P. C. Lacaze, *Synthetic Metals* **1998**, *93*, 133–142. http://dx.doi.org/10.1016/S0379-6779(97)04099-X
25. J. L. Camalet, J. C. Lacroix, S. Aeiyach, K.Chane-Ching, P. C. Lacaze, J. Electroanal. Chem. 1996, 416, 179–182. http://dx.doi.org/10.1016/S0022-0728(96)01012-1
26. A. T. Ozyilmaz, A. Akdag, I. H. Karahan, G. Ozyilmaz, *Progress in Organic Coatings.* **2013**, *76*, 993–997. http://dx.doi.org/10.1016/j.porgcoat.2012.10.020
27. J. B. Bajat, S. Stanković, B. M. Jokić, *J. Solid State Electrochem*. **2009**, *13*, 755–762. http://dx.doi.org/10.1007/s10008-008-0604-5
28. V. B. Miskovic-Stankovic, J. B. Zotovic, Z. Kacarevic-Popovic, M.D. Maksimovic, *Electrochimica Acta*. **1999**, *44*, 4269–4277. http://dx.doi.org/10.1016/S0013-4686(99)00142-5
29. J. B. Bajat, Z. Kacarevic-Popovic, V. B. Miskovic-Stankovic, M. D. Maksimovic, *Progress in Organic Coatings.* **2000**, *39*, 127–135. http://dx.doi.org/10.1016/S0300-9440(00)00127-2
30. T. Adaniya, T. Hara, M. Sagiyama, T. Homa, T. Watanabe, *Plating and Surface Finishing*. **1985**, *72*, 52–56.
31. S. Amirat, R. Rehamnia, M. Bordes, J. Creus, *Mater. Corros.* **2013**, *64*, 328–334. http://dx.doi.org/10.1002/maco.201106290
32. N. Eliaz, K. Venkatakrishna, A. Chitharanjan Hedge, *Surface & Coatings Technol.* **2010**, *205*, 1969–1978. http://dx.doi.org/10.1016/j.surfcoat.2010.08.077
33. J. Winiarski, W. Tylus, B Szczygiel, *Appl. Surface Sci*. **2016**, *364*, 455–466. http://dx.doi.org/10.1016/j.apsusc.2015.12.183
34. N. M. Martyak, P. Mc Andrew, J. E. McCaskie, D. Dijon, *Progress in Organic Coatings* **2002**, *45*, 23–32. http://dx.doi.org/10.1016/S0300-9440(02)00070-X
35. A. T. Ozyilmaz, A. Akdag, Transactions of the Institute of Metal Finishing **2013**, *91*, 44–51. http://dx.doi.org/10.1179/0020296712Z.00000000063
36. A. T. Ozyilmaz, A. Akdag, Transactions of the Institute of Metal Finishing **2011**, *89*, 215–224. http://dx.doi.org/10.1179/174591911X13077162170188
37. G. W. Walter, *Corrosion Sci.* **1986**, *26(9)*, 681–703. http://dx.doi.org/10.1016/0010-938X(86)90033-8
38. F. Mansfeld, J. Appl. Electrochem. **1995**, *25*, 187–202.

Povzetek

Plasti cink-železo (Zn-Fe) in cink-železo-kobalt (Zn-Fe-Co) so bile nanešene na elektrode iz ogljikovega jekla z uporabo toka 3 mA. Z uporabo natrijevega oksalata oziroma natrijevega tartrata kot medija, smo z elektrodepozicijo nanesli pasivne plasti oksalata oziroma tartrata na ogljikovo jeklo ter na ogljikovo jeklo s plastmi Zn-Fe in Zn-Fe-Co. SEM posnetki so pokazali različne strukture pasivnih plasti na ogljikovem jeklu in ogljikovem jeklu s Zn-Fe in Zn-Fe-Co zlitinami. Korozijski testi materiala so pokazali, da je korozijska zaščita materiala boljša v primeru plasti Zn-Fe-Co, kot pri uporabi Zn-Fe zlitine. Po drugi strani pa oksalatne plasti na elektrodah iz ogljikovega jekla in na elektrodah s plastmi Zn-Fe in Zn-Fe-Co zlitin nudijo boljšo korozijsko zaščito kot tartratne plasti.